OXFORD
SOT | Society of Toxicology
www.toxsci.oxfordjournals.org

TOXICOLOGICAL SCIENCES, 141(1), 2014, 263–277

doi: 10.1093/toxsci/kfu124
Advance Access Publication Date: June 27, 2014

Tolerance to Acetaminophen Hepatotoxicity in the Mouse Model of Autoprotection Is Associated with Induction of Flavin-Containing Monooxygenase-3 (FMO3) in Hepatocytes

Swetha Rudraiah*, Philip R. Rohrer*, Igor Gurevich†, Michael J. Goedken‡, Theodore Rasmussen*, Ronald N. Hines§, and José E. Manautou*,1

*Department of Pharmaceutical Sciences, University of Connecticut, Storrs, Connecticut 06269, †Cellular Dynamics International, Madison, Wisconsin 53711, ‡Rutgers University, Office of Translational Science, New Brunswick, New Jersey 08901 and §US EPA, National Health and Environmental Effects Research Laboratory, Research Triangle Park, North Carolina 27711

[1]To whom correspondence should be addressed at Toxicology Program, Department of Pharmaceutical Sciences, School of Pharmacy, University of Connecticut, 69 North Eagleville Road, Unit 3092, Storrs, CT 06269-3092. Fax: (860) 486-5792. E-mail: jose.manautou@uconn.edu.

ABSTRACT

Acetaminophen (APAP) pretreatment with a hepatotoxic dose (400 mg/kg) in mice results in resistance to a second, higher dose (600 mg/kg) of APAP (APAP autoprotection). Recent microarray work by our group showed a drastic induction of liver flavin containing monooxygenase-3 (Fmo3) mRNA expression in our mouse model of APAP autoprotection. The role of liver Fmo3, which detoxifies xenobiotics, in APAP autoprotection is unknown. The purpose of this study was to characterize the gene regulation and protein expression of liver *Fmo3* during APAP hepatotoxicity. The functional consequences of *Fmo3* induction were also investigated. Plasma and livers were collected from male C57BL/6J mice over a period of 72 h following a single dose of APAP (400 mg/kg) to measure Fmo3 mRNA and protein expression. Although Fmo3 mRNA levels increased significantly following APAP treatment, protein expression changed marginally. In contrast, both Fmo3 mRNA and protein expression were significantly higher in APAP autoprotected livers. Unlike male C57BL/6J mice, female mice have ~80-times higher constitutive Fmo3 mRNA levels and are highly resistant to APAP hepatotoxicity. Coadministration of APAP with the FMO inhibitor methimazole rendered female mice susceptible to APAP hepatotoxicity, with no changes in susceptibility detected in male mice. Furthermore, a human hepatocyte cell line (HC-04) clone over-expressing human FMO3 showed enhanced resistance to APAP cytotoxicity. Taken together, these findings establish for the first time induction of Fmo3 protein expression and function by xenobiotic treatment. Our results also indicate that Fmo3 expression and function plays a role in protecting the liver from APAP-induced toxicity. Although the mechanism(s) of this protection remains to be elucidated, this work describes a novel protective function for this enzyme.

Key words: acetaminophen; autoprotection; Fmo3; hepatotoxicity; inhibitor; methimazole

Acetaminophen (APAP) overdose is a leading cause of acute liver failure in the United States and Great Britain, accounting for >50% of all acute liver failure cases from all etiologies (Larson *et al.*, 2005; Lee, 2010). APAP is safe at therapeutic doses, where the majority of APAP administered is glucuronidated or sulfated and the metabolites are safely excreted into the urine and bile. Under these conditions, a small amount of APAP also undergoes bioactivation by cytochrome P450 metabolism to generate *N*-acetyl-*p*-benzoquinone imine (NAPQI), a reactive metabolite that can be detoxified by hepatic glutathione (GSH). However,

when NAPQI is produced in large amounts, as in the case of APAP overdose, GSH stores are depleted and NAPQI reacts with intracellular thiols, binds covalently to cellular macromolecules, and produces oxidative stress, which ultimately results in necrosis of centrilobular hepatocytes (Cohen *et al.*, 1997; Hinson *et al.*, 2010). The growing concern over APAP-induced hepatotoxicity, has prompted extensive research aimed at devising measures to reduce the risk of APAP heptotoxicity.

An experimental approach to modulate APAP hepatotoxicity in rodents is through auto/heteroprotection. Autoprotection is resistance to toxicant re-exposure following acute, mild injury with the same toxicant, whereas in heteroprotection, the initial toxicant used is different from the second. Mehendale *et al.* first demonstrated autoprotection in rats in early 1990s with carbon tetrachloride (CCl_4) (Thakore and Mehendale, 1991). Previous studies conducted in our laboratory have demonstrated both auto/heteroprotection in mice and that pretreatment with various chemicals can reduce the severity of APAP toxicity in mice (Aleksunes *et al.*, 2008; Manautou *et al.*, 1994). For instance, Manautou *et al.* (1994) showed that peroxisome proliferators such as clofibrate at subtoxic doses protect rodents from APAP toxicity (APAP heteroprotection) (Manautou *et al.*, 1994). Alternatively, APAP at a mild toxic dose protects mice against hepatotoxicity from higher doses of APAP (APAP autoprotection) (Aleksunes *et al.*, 2008). This model of APAP autoprotection was used to investigate the role of hepatobiliary drug transporters during the development of resistance to APAP hepatotoxicity. In this study, an increased expression of the sinusoidal efflux transporter Mrp4 (Multidrug resistance-associated protein 4) is evidenced in the hepatocytes localized to centrilobular areas where compensatory hepatocellular proliferation following pretreatment with mildly toxic doses of APAP is confined. The protection is shown to occur independently of changes in bioactivation or detoxification of APAP.

The utility of gene array analysis to address mechanistic toxicology questions has been demonstrated in our lab (Moffit *et al.*, 2007). Even though our previous study demonstrated the role of the drug transporter Mrp4 in APAP autoprotection (Aleksunes *et al.*, 2008), a gene array analysis was performed to identify any other differentially expressed genes resulting from APAP pretreatment that might also contribute to the development of resistance to APAP hepatotoxicity upon re-exposure to this toxicant. Gene array analysis revealed statistically significant gene expression changes unique to the APAP autoprotection mouse model (mice pretreated and re-exposed to APAP) and further analysis of these genes using causal reasoning engine (CRE) provided insights into the signaling pathways involved in autoprotection (O'Connor *et al.*, 2014). Of several noteworthy genes that were identified to be differentially expressed in APAP autoprotected mice, *Fmo3* is one of them. *Fmo3* is unique in a way that it is considered noninducible (Cashman and Zhang, 2002), but Fmo3 mRNA expression increased 20- and 7-fold at 4 and 24 h in the autoprotected group, respectively (O'Connor *et al.*, 2014). Although a role of *Fmo3* in APAP hepatotoxicity is not known, it was the most biologically plausible for playing a role in autoprotection.

Fmo3 is a monooxygenase involved in drug-metabolism somewhat similar to cytochrome P450 (CYP) in that it produces many of the same metabolites, although its substrate specificity is much more limited. Fmo3 is not known to metabolize APAP and most metabolic products of Fmo3 are considered to be nontoxic (Krueger and Williams, 2005). Hepatic expression of the *Fmo3* gene is highly variable showing cell-, tissue-, gender-, and developmental stage-specific expression patterns (Hines, 2006; Janmohamed *et al.*, 2004; Koukouritaki *et al.*, 2002). Mammalian *Fmo3* is also considered to be noninducible (Cashman and Zhang, 2002). However, recent studies by Celius *et al.* showed that activation of the aryl hydrocarbon (Ah) receptor induces Fmo3 mRNA in mice, with marginal changes in protein levels (Celius *et al.*, 2008, 2010). To our knowledge, the current study is only the second to document xenobiotic-dependent *Fmo3* induction, the importance of which is unknown. Further, the role of *Fmo3* in APAP-induced hepatotoxicity and/or autoprotection also is not known. However, it is intriguing that female mice, which contain ~80-times more hepatic Fmo3 mRNA than males (Janmohamed *et al.*, 2004), are much more resistant to APAP hepatotoxicity compared with their male counterparts (Dai *et al.*, 2006).

The initial studies reported herein describe *Fmo3* gene expression during APAP-induced hepatotoxicity. To better understand, an *Fmo3* role in protection against APAP hepatotoxicity, we further attempted to establish a causal relationship between the two, i.e., *Fmo3* gene expression and APAP hepatotoxicity. Thus, the functional significance of *Fmo3* over-expression during APAP hepatotoxicity was evaluated. To date, there are no commercially available *Fmo3*-specific knockout mice because the expression of this enzyme in male mouse liver is switched off during development and male mice are essentially void of Fmo3 protein. In the absence of functional Fmo3 protein in normal male mice, there has been no need for developing a knockout model (Hernandez *et al.*, 2009; Shephard and Phillips, 2010). As an alternative model to low Fmo3 function, inhibition of Fmo3 activity in female mice was achieved using the FMO inhibitor, methimazole. Methimazole (MMI), an antithyroid drug, is an FMO substrate and also a competitive inhibitor that has been used to block FMO-mediated conversion of various compounds in animal models (Nace *et al.*, 1997). Fmo3 and Fmo5 are among the most abundant FMO enzymes in female mouse liver and MMI is not a substrate for Fmo5 (Cherrington *et al.*, 1998; Hines, 2006; Overby *et al.*, 1995; Zhang *et al.*, 2007). Thus, with MMI, among all FMO enzymes, Fmo3 was predominantly inhibited. Taking advantage of this observation, we could test the hypothesis that MMI inhibition of Fmo3 renders female mice susceptible to APAP-induced hepatotoxicity. In addition to the *in vivo* Fmo3 inhibitor study, we also developed an *in vitro* transgene over-expression system. We have established for the first time a stable cell line (human hepatocyte: HC-04) that over-expresses human FMO3 protein. Using this system, we could test the hypothesis that enhanced expression of FMO3 confers resistance against APAP-induced cytotoxicity.

FMO is involved in the oxygenation of sulfur-containing endogenous substrates, e.g., catalyzing the conversion of cysteamine (reduced form) to cystamine (disulfide form) (Poulsen, 1981). Although the physiological role of cysteamine S-oxygenation by Fmo3 is not clear, in the 1970s, Zieglar and Poulsen proposed that oxygenation of cysteamine may be a significant source of disulfide, maintaining the cellular thiol:disulfide potential in a cell (Ziegler *et al.*, 1979). Upregulation of Fmo3 during APAP-induced hepatotoxicity and oxygenation of cysteamine by Fmo3 may serve to help control the overall thiol:disulfide redox state of the cell, which in turn may modulate cellular metabolism and/or activate signal transduction pathways leading to altered susceptibility to APAP (or protection). To reiterate, the objective of the current investigation was to characterize the gene regulation and protein expression of liver Fmo3 during APAP-induced hepatotoxicity. The functional consequences of Fmo3 induction were also investigated. To our

knowledge, this is the first report describing a novel protective function for this drug-metabolizing enzyme.

MATERIALS AND METHODS

Chemicals. Acetaminophen, propylene glycol, methimazole, and reduced GSH were purchased from Sigma-Aldrich (St Louis, MO). All other reagents were of reagent grade or better.

Animals. Male and female C57BL/6J mice (9- to 10-week-old) were obtained from Jackson Laboratories (Bar Harbot, ME). Upon arrival, mice were acclimated for 1 week prior to experimentation. Mice were housed in a 12-h dark/light cycle in a temperature and humidity controlled environment. Mice were fed laboratory rodent diet (Harlan Teklad 2018, Madison, WI) *ad libitum*.

Dosing regimen 1. Following an overnight fast, male mice ($n = 6$) were treated with APAP (400 mg/kg, ip) in 50% propylene glycol (PG) or vehicle. Animals were sacrificed 24, 48, and 72 h after APAP treatment. Plasma and liver were collected for measuring alanine amino transferase (ALT) activity, Fmo3 mRNA and protein levels, and enzyme activity.

Dosing regimen 2. Following an overnight fasting, male mice ($n = 6$) were treated with APAP (400 mg/kg, ip) in 50% PG or vehicle. Animals were treated with APAP (600 mg/kg, ip) in 50% PG or vehicle, 48 h after the first treatment. Animals were sacrificed and plasma and liver were collected after 24 h for analysis.

Dosing regimen 3. Following an overnight fast, female mice ($n = 6$) were administered a single dose of MMI (50 mg/kg, ip) in saline. Animals were sacrificed and plasma and livers were collected at 0.5, 4, 12, and 24 h for analysis of hepatotoxicity and GSH content. A single group of mice received a first dose of MMI (50 mg/kg, ip) and 12 h after the first dose, mice were treated with a second dose of MMI (50 mg/kg, ip). Plasma and liver were collected 12 h later for analysis.

Dosing regimen 4. Following an overnight fasting, female or male mice ($n = 6$) were administered vehicle (saline) or MMI (50 mg/kg, ip). Animals were treated with APAP (400 mg/kg, ip), 30 min later. The group receiving two doses of MMI along with APAP received the first dose of MMI 30 min prior to APAP treatment and the second dose of MMI at 12 h after the first dose. Mice in the group receiving only the second MMI dose were treated with MMI 11.5 h after APAP treatment. At 24 h after APAP treatment, animals were sacrificed and plasma and liver were collected for measuring ALT activity and GSH levels in this group of mice.

All animal studies were performed in accordance with National Institute of Health standards and the *Guide for the Care and Use of Laboratory Animals*. This work was approved by the University of Connecticut's Institutional Animal Care and Use Committee.

Alanine aminotransferase (ALT) assay. Plasma ALT activity was determined as a biomarker of hepatocellular injury. Infinity ALT Liquid Stable Reagent (Thermo Fisher Scientific Inc., Waltham, MA) was used to determine ALT activity. Samples were analyzed using a Bio-Tek Power Wave X Spectrophotometer.

RNA isolation and quantitative real-time polymerase chain reaction (qRT-PCR). TRIzol reagent (Life Technologies, Carlsbad, CA) was used to extract total mouse liver RNA. cDNA was then made using an M-MLV RT kit (Invitrogen, Carlsbad, CA). Fmo3 mRNA expression was quantified by the ΔΔCT method and normalized to two housekeeping genes, β-actin and ribosomal protein S18. Data presented in this paper were normalized to β-actin. Primer pairs were synthesized by Integrated DNA Technologies (Coralville, IA) and are as follows: Fmo3 forward: 5′-GGA AGA GTT GGT GAA GAC CG-3′, reverse: 5′-CCC ACA TGC TTT GAG AGG AG-3′. Amplification was performed using an Applied Biosystems 7500 Fast Real-Time PCR System. Amplification was carried out in a 20-μl reaction volume containing 8 μl diluted cDNA, Fast SYBR Green PCR Master Mix (Applied Biosystems, Foster City, CA) and 1 μM of each primer.

Preparation of crude membrane and microsomal fractions. Microsomes were isolated from livers as described previously (Cashman and Hanzlik, 1981). Briefly, livers were homogenized in cold homogenization buffer (0.1M potassium phosphate, 0.1mM dithiothreitol (DTT), 2% sucrose, pH 9.0) and homogenates were centrifuged at 10,000 × g for 20 min at 4°C. The supernatant was then centrifuged at 100,000 × g for 60 min. The resulting pellet was washed and resuspended in 0.1 M potassium phosphate buffer (pH 9.0) containing 1 mM EDTA and stored at −80°C. Protease inhibitor was added to all buffers before use. Protein concentration was determined by the method of Lowry using Bio-Rad protein assay reagents (Bio-Rad Laboratories, Hercules, CA).

Western blot analysis. For Western blot analysis of Fmo3, microsomal proteins (10 μg) were electrophoretically resolved using 10% polyacrylamide gels and transferred onto PVDF-Plus membrane (Micron Separations, Westboro, MA). A custom-made rabbit anti-mouse Fmo3 primary antibody (GenScript USA Inc., NJ) was used to detect Fmo3 with β-actin as a loading control. Extensive characterization of the reactivity and/or specificity of this antibody was carried out. The antibody developed was specific for mouse Fmo3 protein. Blots were then incubated with horseradish peroxidase (HRP) conjugated secondary antibodies against rabbit IgG. Protein-antibody complexes were detected using a chemiluminescent kit (Thermo Scientific, IL) followed by exposure to X-ray film.

Enzyme assay. MMI metabolism was determined spectrophotometrically by measuring the rate of MMI S-oxygenation via the reaction of the oxidized product with nitro-5-thiobenzoate (TNB) to generate 5,5′-dithio-bis(2-nitrobenzoate) (DTNB). The incubation mixture consisted of 50 mM sodium phosphate buffer (pH 9.0), 0.5 mM NADP+, 0.5 mM glucose-6-phosphate, 1.5 IU/ml glucose-6-phosphate dehydrogenase, 0.06 mM DTNB, 0.04 mM dithiothreitol, and 100–150 μg/ml liver microsomes isolated from mice. Reactions were initiated by the addition of different amounts of MMI (substrate) and range of MMI concentrations used were between 1.25 and 800 μM. Incubations were done in duplicates. The disappearance of the yellow color was measured spectrophotometrically at 412 nM and specific activity (μM/min/mg) was determined using the molar extinction coefficient of NADPH (28.2 mM^{-1} cm^{-1}).

Immunohistochemistry. Immunohistochemical detection of Fmo3 protein was performed on 5 μm liver sections from tissues fixed in 10% neutral-buffered zinc formalin followed by routine processing, paraffin embedding, sectioning, and rehydration. Antigen retrieval was performed via microwave (950 W) method in 10 mM sodium citrate buffer for 2 min at 100% power and at 30% power for another 8 min. Endogenous peroxidase activity was blocked with a 10-min incubation in 3% H_2O_2, and avidin/biotin blocking was performed using a commercially available kit from Vector Laboratories (Burlingame, CA). Sections were incubated overnight with the previously mentioned antimouse Fmo3 primary antibody at a dilution of 1:8000 followed by Vector Laboratory's biotinylated goat anti-rabbit secondary antibody for 30

min. Protein-antibody complexes were detected with the Vector Elite ABC reagent and developed using a Vector Nova RED substrate kit for peroxidase. Slides were counterstained with hematoxylin, and mounted in "Protocol" mounting media (Fisher Scientific).

GSH assay. Total hepatic GSH concentrations were determined by the recycling method as previously described (Rahman *et al.*, 2006). Briefly, 15–25 mg of liver tissue was added to 500 μl of 5 mM EDTA disodium salt in 0.1 M potassium phosphate buffer containing protease inhibitors. Tissues were kept on ice and homogenized by hand in a dounce homogenizer for 5–6 strokes. Equal volumes of 0.67 mg/ml DTNB and 3.3 units/ml glutathione reductase (Sigma-Aldrich) in 0.1 M potassium phosphate buffer containing 5mM EDTA disodium salt were mixed and 120 μl was added to 20 μl of each liver homogenate in a 96-well plate. Sixty microliters of 0.67 mg/ml β-NADPH (Sigma) in 0.1 M potassium phosphate buffer containing 5 mM EDTA disodium salt was then added to each well. Absorbance was read immediately at 412 nm, taking measurements every 30 s for 2 min. The assay was performed in duplicate for each sample and compared with a standard curve made from two-fold serial dilutions (211.2–1.65 nmol/ml) of a GSH standard (Sigma).

Histopathology. Liver samples were fixed in 10% neutral-buffered zinc formalin prior to processing and paraffin embedding. Liver sections (5 μm) were stained with hematoxylin and eosin (H&E). Sections were examined by light microscopy for the presence and severity of necrosis and degeneration using an established grading system (Manautou *et al.*, 1994).

Lentiviral vector construction. The *FMO3*-T2A-luc lentiviral transfer vector was constructed by modifying the FUdeltaGW-rtTA (obtained from K. Hochedlinger via Addgene, Cambridge, MA, plasmid 19780) to replace the rtTA insert with a polylinker designed to accommodate the human *FMO3* ORF (Clone ID: 5175615 from Open Biosystems, Waltham, MA). To allow for bicistronic expression of *FMO3* and luciferase, sequence encoding the T2A peptide (Szymczak *et al.*, 2004) was inserted into the polylinker. The luciferase ORF from pGL4.10 vector (Promega, Madison, WI) was cloned in frame with FMO3 and the T2A sequence. Luciferase activity was used to normalize levels of FMO3 overexpression.

Cell culture and transduction. The replication-defective virus was generated in HEK 293T cells and concentrated as previously described (Maherali *et al.*, 2008). HC-04 cells were seeded 24 h prior to transduction in complete dulbecco's modified eagle's medium (DMEM) and then infected with a series of volumes of untitered concentrate (100, 50, and 25 μl per well of a 6-well culture dish) overnight. Prior to, during, and after the viral transduction, the cells were maintained in complete DMEM containing 0.05 mM riboflavin. Media was changed daily to prevent riboflavin degradation.

Cell culture and treatment. HC-04 cells overexpressing human FMO3 (hFMO3-HC-04) and empty vector (EV-HC-04) were maintained in DMEM supplemented with 10 mM glucose, 10% fetal bovine serum (FBS), 0.05 mM riboflavin and 1% antibiotic-antimycotic (100 units/ml penicillin G sodium, 100 μg/ml streptomycin sulfate, and 0.25 μg/ml amphotericin B) in a 5% CO_2 and humidified environment (95% relative humidity) at 37°C. For APAP treatments, cells were seeded at 200,000 cells per well in a 24-well plate. The following day, culture media was replaced with media containing APAP (1–15 mM). Twenty-four hours later, cytotoxicity was measured by the LDH assay. For MMI treatments, cells were seeded at 200,000 cells per well in a 24-well plate. The next day, cells were incubated in media containing 1 mM MMI for 30 min at 37°C. Thirty minutes following incubation with MMI, culture media containing 15 mM APAP was added to wells. Cytotoxicity was measured using the LDH assay 24 h later.

LDH leakage. As a measure of cytotoxicity following APAP treatment, percentage LDH leakage in all *in vitro* experiments was determined via the Tox-7 kit. The assay was performed according to manufacturer's instructions (Sigma-Aldrich).

Statistical analysis. Results are expressed as means ± standard error (SE). Data were analyzed using the Student's *t*-test or ANOVA followed by a *post hoc* test. Although Student's *t*-test was used to compare means of two different treatment groups, ANOVA was used to compare the means of more than two means of different treatment groups that are normally distributed with a common variance. Differences were considered significant at $p < 0.05$.

RESULTS

Time Course of Plasma ALT Activity and Fmo3 mRNA Levels After APAP Treatment

Administration of 400 mg/kg APAP to male C57Bl/6J mice resulted in elevation of plasma ALT levels (Fig. 1A). Plasma ALT activity increased to 191 ± 18 and 219 ± 47 IU/l at 24 and 48 h, respectively, following APAP treatment (mean plasma ALT activity in control mice was 25 ± 5 IU/l). By 72 h, plasma ALT activity is not statistically different from propylene glycol vehicle controls indicating recovery from APAP-induced liver injury. Fmo3 mRNA levels were quantified by qRT-PCR. The results in Figure 1B show that Fmo3 mRNA levels increased by 5 ± 2.6- and 23 ± 5.6-fold, at 24 and 48 h, respectively compared with the 0 h control group.

Time Course of Fmo3 Protein Expression After APAP Treatment

To examine the temporal changes in *Fmo3* gene expression and function following APAP treatment, Fmo3 protein levels were quantified by Western blotting and by measuring catalytic activity using MMI as substrate. Representative blots and associated densitometric analysis are shown in Figures 2A and 2B, respectively. Although the expression of Fmo3 protein tended to increase by 1.1 ± 0.3- to 1.6 ± 0.2-fold between 24 and 72 h after APAP, these increases are statistically significant only at 72 h. An alternative method to quantitate Fmo3 protein induction is by measuring FMO catalytic activity using MMI (Zhang *et al.*, 2007). With APAP treatment, FMO-specific activity increased over time and this increase is statistically significant at 72 h only (24 ± 1.5 μM/min/mg) (Fig. 2C). Figure 2D shows immunohistochemical analysis of Fmo3 protein localization. Cellular localization of Fmo3 protein and degree of protein expression did not change at 24 or 48 h, but marginally increased at 72 h after treatment with a single dose APAP (400 mg/kg). Unlike Fmo3 mRNA levels that peaked at 48 h, maximum Fmo3 protein expression is observed at 72 h following APAP treatment. These data demonstrate that a single dose APAP (400 mg/kg) treatment results in a marginal, yet significant increase in Fmo3 protein levels and activity at 72 h, the longest timepoint tested.

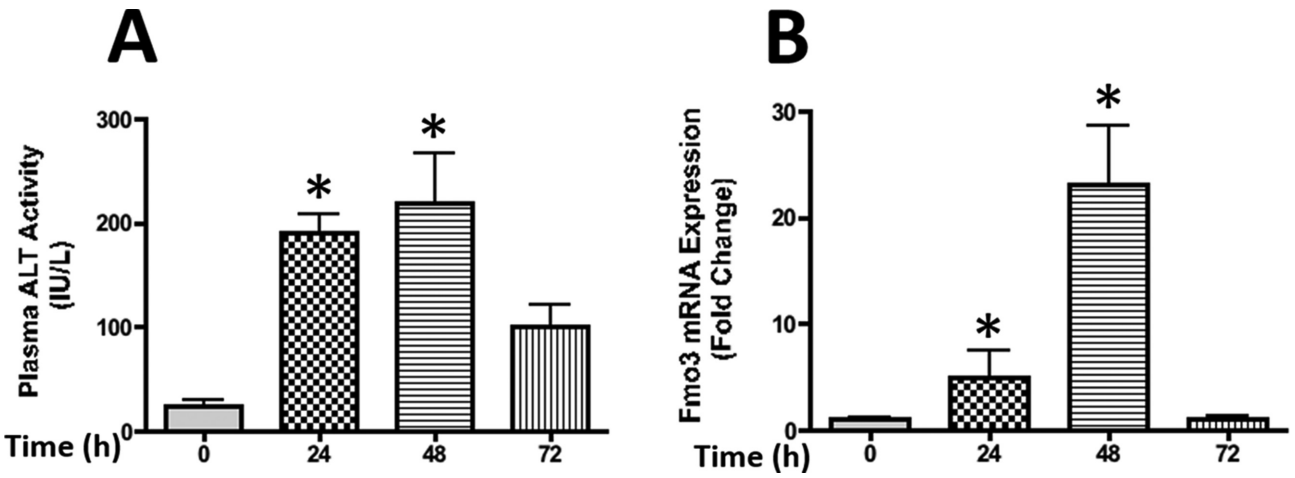

FIG. 1. Plasma ALT activity and quantitative RT-PCR analysis of liver Fmo3 transcripts following a single dose APAP treatment. Plasma and livers were collected from mice 24, 48 and 72 h following APAP (400 mg/kg) or vehicle treatments. (A) The data are presented as mean plasma ALT (IU/l) ± SE. (B) RNA was isolated from livers and further cDNA was made using a commercial MMLV-RT kit. The cDNA samples were analyzed by quantitative RT-PCR using Fmo3 mouse-specific primers. Gene expression was normalized to housekeeping gene β-actin. Fmo3 mRNA expression are presented as mean fold change ± SE. One-way ANOVA was performed followed by the Dunnett's *post hoc* test. Asterisks (*) represent a statistical difference ($p < 0.05$) between 0 h vehicle and APAP-treated groups.

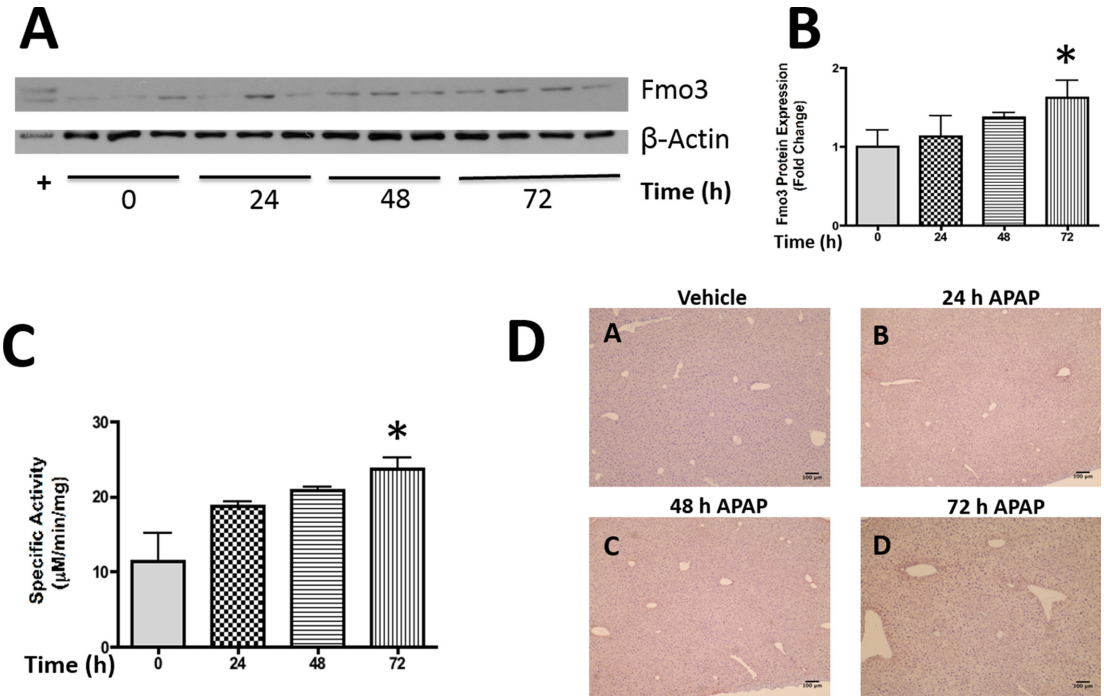

FIG. 2. Analysis of liver Fmo3 protein expression following a single dose APAP treatment by Western blotting, enzyme activity assay as well as by immunohistochemistry. After overnight fasting, mice received a single dose of 400 mg/kg APAP or vehicle. Livers were collected at 24, 48, and 72 h following APAP or vehicle treatments. Western blots for Fmo3 were performed using liver microsomes from control and APAP-treated mice. A custom-made rabbit anti-mouse Fmo3 primary antibody, described in the Materials and Methods section was used to detect Fmo3. Equal protein loading (10 μg protein/lane) was confirmed by detection of β-actin. Microsomal protein isolated from naïve female mouse liver was used as a positive control indicated by "+" sign. The data are presented as blots (A) and as mean Fmo3 protein expression (fold change) ± SE (B). FMO activity was measured in liver microsomes from control and APAP-treated mice using methimazole as substrate as described under Materials and Methods section. Data are presented as mean specific activity (μM/min/mg) ± SE (C). Asterisks (*) represent a statistical difference ($p < 0.05$) between 0 h vehicle and APAP-treated groups. Immunohistochemical staining to detect Fmo3 was conducted on zinc formalin fixed, paraffin-embedded liver sections from control and APAP-treated mice. Immunochemical staining was performed with the same antibody used for Western blotting. Representative images are shown (D). Scale bar: 100 μm. (A) Vehicle-treated 0 h; (B) APAP-treated 24 h; (C) APAP-treated 48 h; (D) APAP-treated 72 h.

Plasma ALT Activity and Fmo3 mRNA Expression in the Mouse Model of APAP Autoprotection

Previous studies conducted in our laboratory demonstrated the phenomenon of APAP autoprotection in mice, where mice receiving an initial mild toxic dose of APAP are protected against hepatotoxicity from higher doses (Aleksunes *et al.*, 2008). To investigate *Fmo3* gene expression in the mouse model of APAP autoprotection, male C57BL/6J mice were pretreated with either propylene glycol vehicle or 400 mg/kg APAP. Forty-eight hours following pretreatment, mice were challenged with vehicle or a higher dose of APAP (600 mg/kg). Plasma ALT activity and Fmo3 mRNA levels were measured 24 h after the challenge dose (Figs. 3A and 3B, respectively). Plasma ALT levels in mice receiving vehicle pretreatment and APAP challenge (600 mg/kg; VA) increased significantly to 1600 ± 413 IU/l compared with vehicle controls (VV). Likewise, ALT levels in mice pretreated and challenged with APAP (AA; autoprotected group) increased significantly to 230 ± 69 IU/l compared with VV controls. However, the values are significantly lower than in the VA group. Consistent with the single dose APAP (400 mg/kg) study, APAP pretreated, vehicle challenged mice (AV) have marginal increases in ALT values in comparison to VV controls. The results in Figure 3B show Fmo3 mRNA levels in the mouse model of APAP autoprotection. Fmo3 mRNA transcript levels in the AV and AA groups increased significantly by 39 ± 5- and 70 ± 11-fold, respectively, with APAP autoprotected mice showing the greatest (70-fold) induction.

Fmo3 Protein Expression in the Mouse Model of APAP Autoprotection

Fmo3 protein expression is not normally detectable in adult male mice livers because the expression of this enzyme is silenced during development (Cherrington *et al.*, 1998; Falls *et al.*, 1997; Shephard and Phillips, 2010). To determine if Fmo3 protein expression correlates with the mRNA expression seen in APAP autoprotected male mouse livers, Western blot analysis was performed as described in the Materials and Methods section. Representative blots are shown in Figure 4A and densitometric analysis of blots are shown in Figure 4B. As expected, no detectable hepatic Fmo3 protein is present in VV control livers. Following treatment with APAP (dosing regimen 2) Fmo3 protein levels increased in both AV (p-value: 0.0743) and AA group (p-value: 0.041). However, the elevation is statistically significant only in APAP autoprotected group (15 ± 2-fold change). In agreement with protein expression data, the MMI assay used to measure enzyme-specific activity shows an increase in activity to 16 ± 2 and 42 ± 5 μM/min/mg in AV and AA groups of mice, respectively, compared with vehicle controls (3 ± 1 μM/min/mg) (Fig. 4C). Figure 5 shows immunohistochemical analysis of Fmo3 protein localization. Protein staining is localized to centrilobular regions in both APAP pretreated and autoprotected livers instead of its conventional periportal localization seen in nontreated female livers. This distinct zonal localization by APAP coincides with the area where damage and/or hepatocellular compensatory repair/proliferation occurs (Figs. 5E/F and 5G/H, respectively).

Effect of Methimazole Treatment on Liver in Mice

Methimazole is a drug used in the treatment of hyperthyroidism and is a high affinity substrate and effective competitive inhibitor of the Fmo-mediated oxidation of various compounds (Nace *et al.*, 1997). Later studies described in this paper use MMI (50 mg/kg) to inhibit FMO activity in female as well as male mice. MMI at higher doses can by itself deplete hepatic GSH levels or cause hepatotoxicity in GSH-depleted mice (Mizutani *et al.*, 1999, 2000). To determine whether administration of MMI by itself at doses used in our study results in hepatotoxicity, female mice were administered either one or two doses of 50 mg/kg MMI. Animals were sacrificed and plasma and livers were collected over a timecourse of 12 h for liver toxicity analysis (dosing regimen 3). Plasma ALT activity increased to 39 ± 4 IU/l at 12 h following a single dose MMI treatment compared with vehicle controls (15 ± 3 IU/l) (Fig. 6A). Even though the ALT activity increased significantly at 12 h, these levels are below the normal physiological range for hepatotoxicity (40–43 IU/l, as per the "Physiological Data Summary" provided by The Jackson Laboratory for female C57BL/6J mice). Hepatic GSH levels are shown in Figure 6B. GSH levels in livers from MMI-treated mice are not different from that in their vehicle-treated controls. In support of ALT activity data, histopathological analysis of H&E stained liver sections from MMI-treated mice do not show any signs of liver injury (Fig. 6C). Collectively these data suggest that MMI at two doses of 50 mg/kg does not result in hepatotoxicity nor does it deplete hepatic GSH levels, one of the key detoxification mechanisms involved during APAP exposure.

Immunohistochemical Analysis of Liver Fmo3 Protein Expression and Localization in Naïve C57BL/6J Male and Female Livers

Female mice express about 80 times higher Fmo3 mRNA levels compared with males (Janmohamed *et al.*, 2004). To examine whether the differences in mRNA levels translate to protein levels, an immunohistochemical analysis for Fmo3 protein expression was performed in naïve livers from male and female mice using our custom-made Fmo3 primary antibody. Consistent with the literature, Fmo3 protein expression and its cellular localization is not detectable in male liver under basal conditions. Strikingly, female livers express higher Fmo3 protein levels compared with male mice. This Fmo3 expression is restricted to hepatocytes surrounding portal veins (Fig. 7).

Effect of Methimazole Treatment on APAP-induced Liver Injury in Female and Male C57BL/6J Mice

As shown in Figure 7, female mice express higher Fmo3 protein levels compared with their male counterparts. It has also been demonstrated that female mice are much more resistant to APAP hepatotoxicity compared with male mice (Dai *et al.*, 2006). If Fmo3 plays a role in conferring tolerance to APAP-induced hepatotoxicity in female mice, methimazole (FMO inhibitor) treatment should render female mice susceptible to APAP hepatotoxicity. To investigate the effect of MMI treatment on APAP-induced hepatotoxicity in female mice, groups of mice received APAP along with either one or two doses of MMI (dosing regimen 4). Plasma ALT activity in female mice did not change compared with vehicle controls following APAP (400 mg/kg) treatment (Fig. 8A) (mean plasma ALT activity in control mice: 27 ± 2 IU/l). APAP treatment along with the first and second dose of MMI (1 and 2 MMI/APAP), significantly increased plasma ALT levels to 3343 ± 802 IU/l. APAP treatment with only the first dose (1 MMI/APAP) of MMI also increased plasma ALT values to 473 ± 93 IU/l. Hepatic GSH levels also are shown in Figure 8B. Liver GSH content measured at 24 h in mice receiving APAP alone show a rebound increase to 72 ± 3 nmol/mg protein compared with vehicle controls (48 ± 4 nmol/mg protein). On the other hand, all three groups of mice receiving APAP and MMI cotreatment show significantly lower GSH levels (1 and 2 MMI/APAP: 19 ± 7, 1 MMI/APAP: 30 ± 3 and APAP/2 MMI: 37 ± 2 nmol/mg protein) compared with the group receiving APAP alone. This change correlates well with higher plasma ALT activity in these three groups. The severity of hepatocellular necrosis by APAP along with MMI was analyzed and graded using a scale ranging from 0

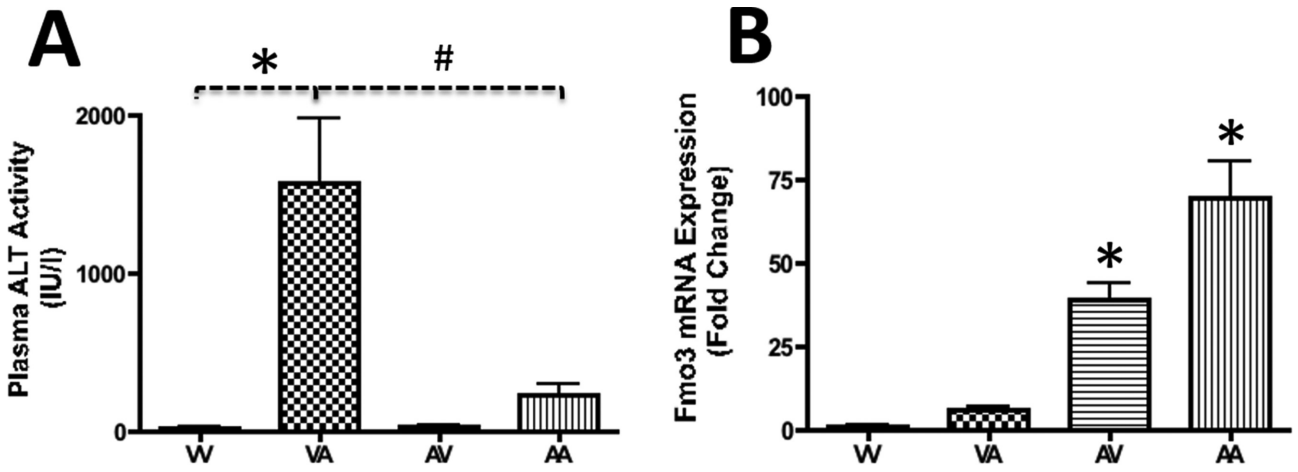

FIG. 3. Plasma ALT activity in the mouse model of APAP autoprotection. Groups of mice were treated with vehicle or APAP 400 mg/kg. Forty-eight hours after pretreatment, mice were challenged with vehicle or APAP 600 mg/kg. Plasma and livers were collected 48 h following APAP challenge. (A) The data are presented as mean plasma ALT (IU/l) ± SE. One-way ANOVA was performed followed by the Dunnett's *post hoc* test. Although asterisks (*) represent a statistical difference ($p < 0.05$) between VV group and VA groups, hash (#) represent a statistical difference ($p < 0.05$) between VA and AA groups. (B) RNA was extracted from livers and cDNA was prepared using a commercial MMLV-RT kit as described in the Materials and Methods section. The cDNA samples were analyzed for Fmo3 mRNA levels by quantitative RT-PCR using Fmo3 mouse-specific primers. Gene expression was normalized to housekeeping gene β-actin. Fmo3 mRNA expression are presented as mean fold change ± SE. One-way ANOVA was performed followed by the Dunnett's *post hoc* test. Asterisks (*) represent a statistical difference ($p < 0.05$) from VV groups and hash (#) represent a statistical difference ($p < 0.05$) between VA and AA groups.

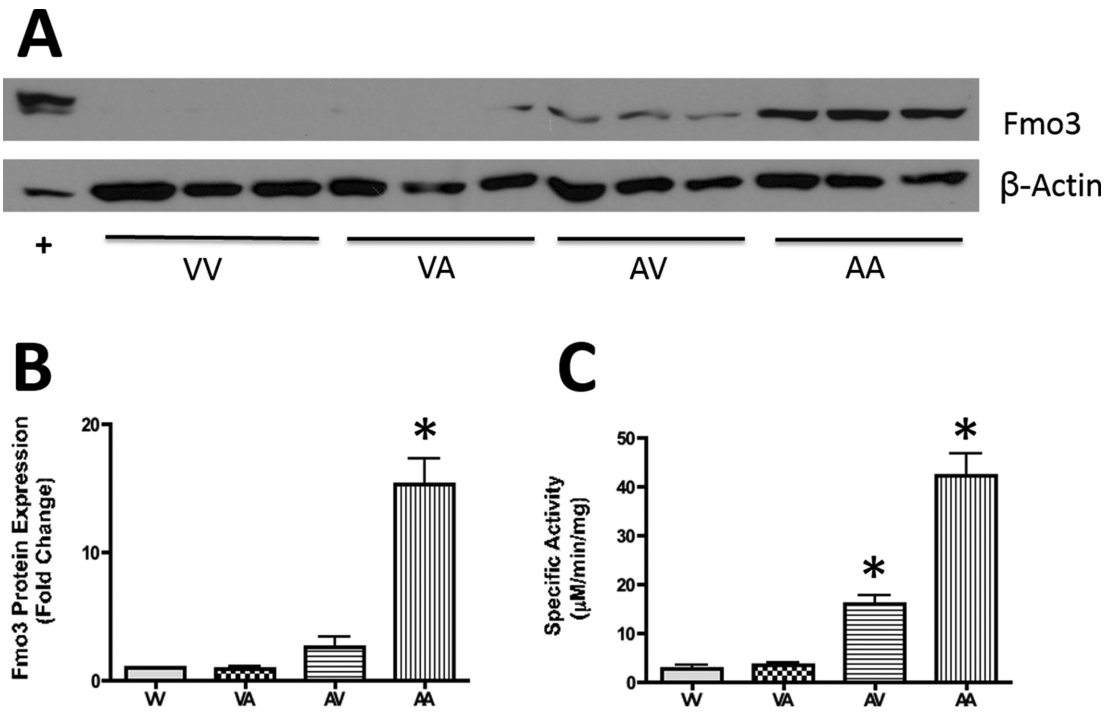

FIG. 4. Analysis of liver Fmo3 protein expression in the mouse model of APAP autoprotection by Western blotting and enzyme activity assay. Dosing regimen is described in detail in the Materials and Methods section. Briefly, groups of mice were administered with vehicle or APAP (400 mg/kg) and 48 h later challenged with vehicle or APAP (600 mg/kg). Livers were collected 24 h following the last treatment. Western blots for Fmo3 was performed using liver microsomes from all groups of mice. A custom-made rabbit anti-mouse Fmo3 primary antibody, described before was used to detect Fmo3. Equal protein loading (10 μg protein/lane) was confirmed by detection of β-actin. Microsomal protein isolated from naïve female mouse liver was used as a positive control indicated by "**+**" sign. The data are presented as blots (A) and as mean Fmo3 protein expression (fold change) ± SE (B). Liver microsomes isolated from all groups of mice were used to measure FMO activity using methimazole as substrate. Data are presented as mean specific activity (μM/min/mg) ± SE (C). Asterisks (*) represent a statistical difference ($p < 0.05$) from VV groups.

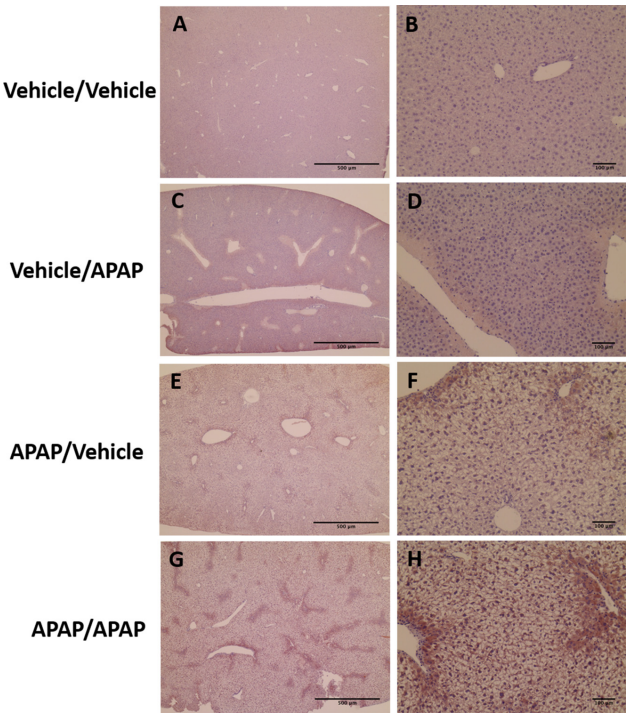

FIG. 5. Immunohistochemical analysis of liver Fmo3 protein expression and localization in the mouse model of APAP autoprotection. Details of APAP autoprotection treatment regimen are described in the Materials and Methods section. Groups of mice were pretreated with vehicle or APAP (400 mg/kg) and challenged with vehicle or APAP (600 mg/kg) 48 h later. Twenty-four hours after the challenge dose livers were collected and fixed in zinc formalin and paraffin embedded. Immunochemical staining to detect Fmo3 was performed with the same antibody used for Western blotting. Representative images from all groups of mice are shown at two magnifications. Scale bar: 100 and 500 μm. (A/B) VV: vehicle pretreated and vehicle challenge group; (C/D) VA: vehicle pretreated and APAP (600 mg/kg) challenge group; (E/F) AV: APAP (400 mg/kg) pretreated and vehicle challenge group; (G/H) AA: APAP (400 mg/kg) pretreated and APAP (600 mg/kg) challenge group liver sections.

to 5. Liver samples with grades >2 are considered to have significant injury (Manautou *et al.*, 1994). Results of histopathological analysis are presented in Figure 8C and Table 1. Examination of liver sections from the control group revealed normal histology. Consistent with the plasma ALT activity, APAP (400 mg/kg) treatment resulted in a minimal amount of hepatocellular injury in female mice. Even though the severity of APAP-related injury increased with MMI, there is greater injury with two doses of MMI.

Fmo5 and Fmo3 are abundant FMO enzymes in female adult mouse liver (Cherrington *et al.*, 1998; Hines, 2006; Janmohamed *et al.*, 2004). Although Fmo3 is abundant in female mice, male mice are void of Fmo3 (Cherrington *et al.*, 1998; Hines, 2006; Janmohamed *et al.*, 2004). With the exception of FMO5, MMI is a substrate for all FMO enzymes (Overby *et al.*, 1995; Zhang *et al.*, 2007). Thus, with MMI we presume female hepatic Fmo3 is predominantly inhibited. If the susceptibility of female mice to APAP-induced hepatotoxicity is due to MMI inhibition of Fmo3 (demonstrated in Fig. 8A and 8B), then we anticipate seeing no alteration in the susceptibility of male mice to APAP hepatotoxicity with MMI administration. To investigate the effect of MMI treatment on APAP-induced hepatotoxicity in male mice, groups of mice received APAP along with either one or two doses of MMI (dosing regimen 4). Administration of APAP (400 mg/kg) in saline to male mice resulted in an elevation of plasma ALT levels to 1794 ± 222 IU/l compared with vehicle controls (45 ± 12 IU/l) (Fig. 8D). APAP coadministration with MMI did not significantly change plasma ALT activity compared with APAP-treated male mice (1 and 2 MMI/APAP: 1984 ± 592, 1 MMI/APAP: 2333 ± 126 and APAP/2 MMI: 1530 ± 328 IU/l). Hepatic GSH levels are presented in Figure 8E. Consistent with plasma ALT levels, hepatic GSH content following APAP (400 mg/kg) treatment decreased significantly to 16 ± 2 nmol/mg protein compared with vehicle controls (61 ± 2 nmol/mg protein). Further, GSH levels did not change significantly in all groups of mice that received APAP along with one or two doses of MMI compared with the APAP only group (1 and 2 MMI/APAP: 13 ± 2, 1 MMI/APAP: 11 ± 2 and APAP/2 MMI: 17 ± 1 nmol/mg protein). These data demonstrate that the susceptibility of female mice to APAP-induced hepatotoxicity from MMI treatment is due to inhibition of hepatic Fmo3.

Establishment of Human Hepatocyte Cell Line (HC-04) Over-expressing Human FMO3 (hFMO3-HC-04)

To further evaluate the functional significance of *FMO3* overexpression during APAP hepatotoxicity, we developed a human hepatocyte cell line (HC-04) that over-expresses human *FMO3*. Unlike HepG2 cells, HC-04 cells express CYPs that bioactivate APAP to its toxic metabolite NAPQI and also are susceptible to APAP-induced cellular toxicity (Lim *et al.*, 2007). Thus, this cell line is a good model for studying the protective effects of *FMO3* gene expression during APAP-induced cytotoxicity. *FMO3* was incorporated into a bicistronic vector driven by the ubiquitin-C promoter, which allowed co-expression of *FMO3* and luciferase (LUC) genes in transduced HC-04 cells. We identified five clones that over-expressed human FMO3, of which three were maintained as cell lines. Results from luciferase activity assays used to measure the efficiency of transduction are presented in Figure 9A. The clones expressed a 33 ± 1-, 89 ± 2-, and 455 ± 8-fold change in luciferase activity as compared with the empty vector control (EV-HC-04). For convenience, these clones are named Low- Mid-, and High-FMO3 expressing cell lines, respectively. FMO3 protein expression was confirmed by performing Western blotting using microsomal fractions isolated from EV expressing HC-04 cells and all three FMO3-over-expressing HC-04 clones. Representative blots and densitometric analysis are shown in Figure 9B. Following transduction, Fmo3 protein levels increased by 5 ± 0.1-, 10 ± 0.3-, and 33 ± 0.5-fold in Low-, Mid-, and High-FMO3 expressing HC-04 cells, respectively. The specific activity of over-expressed FMO3 protein increased to 75 ± 1.2, 80 ± 0.7, and 80 ± 0.6 μM/min/mg in Low-, Mid-, and High-FMO3 expressing HC-04 cells, respectively compared with EV-HC-04 controls (5 μM/min/mg) (Fig. 9C).

Effect of APAP Treatment in HC-04 Cells Over-expressing Human FMO3 (hFMO3-HC-04)

Cell culture and treatment is described in detail in the Materials and Methods section. Results are shown in Figure 10. The percentage LDH leakage into the media in Low-FMO3 expressing hFMO3-HC-04 cells in response to 1, 5, 10, and 15 mM APAP treatment is significantly lower (7, 10, 17, and 24%) compared with empty vector controls (8, 13, 23, and 31%), respectively. The amount of LDH leakage does not change in Mid-FMO3 expressing cells and is significantly greater (9, 14, 28, and 42%) in High-FMO3 expressing cells following 1, 5, 10, and 15 mM APAP treatment. Taken together, these data suggest that over-expression of FMO3 protects against APAP-induced cytotoxicity only in Low-FMO3 expressing cells. By contrast, APAP cytotoxicity is aggravated in the High-FMO3 expressing clone.

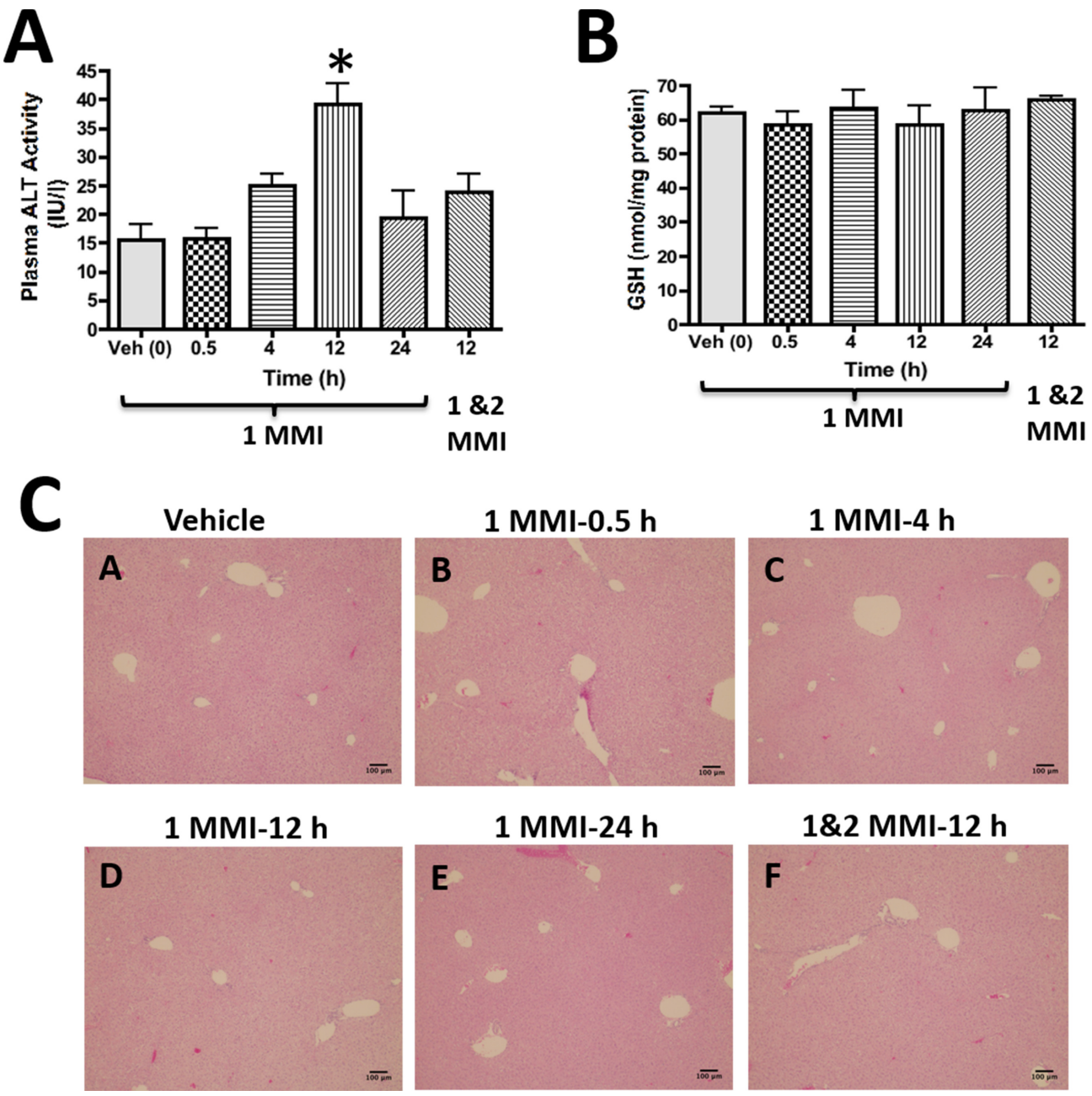

FIG. 6. Plasma ALT activity, hepatic GSH levels and histopathology of liver sections after 50 mg/kg methimazole (MMI) treatment in female mice. Dosing regimen is described in detail in the Materials and Methods section. Briefly, groups of mice were administered a single dose of MMI (50 mg/kg) and plasma and livers were collected 0.5, 4, 12, and 24 h later. A single group of mice received both the first and the second dose of MMI and 12 h after the second dose, plasma and livers were collected for analysis. (A) The data are presented as mean plasma ALT (IU/l) ± SE. (B) GSH levels are expressed as GSH nmol/mg protein ± SE. One-way ANOVA was performed followed by the Dunnett's *post hoc* test. Asterisks (*) represent a statistical difference ($p < 0.05$) between vehicle and MMI-treated groups. (C) Histopathology of formalin-fixed, paraffin-embedded liver sections from MMI-treated mice. Representative images are shown. Scale bar: 100 μm. (A) Control; (B) first dose MMI-treated 0.5 h; (C) first dose MMI-treated 4 h; (D) first dose MMI-treated 12 h; (E) first dose MMI-treated 24 h; (F) first and second dose MMI-treated 12 h.

Effect of MMI Pretreatment during APAP-induced Cytotoxicity in HC-04 Cells Over-expressing Human FMO3 (hFMO3-HC-04)

In response to 15 mM APAP treatment, the percentage LDH leakage into the media in Low-FMO3 expressing cells decreased significantly to 25% compared with EV controls (29%) (Fig. 11). Following pretreatment with 1 mM MMI, the susceptibility of Low-FMO3 expressing cells to APAP-induced cytotoxicity restored to 29%. On the contrary, Mid- and High-FMO3 expressing cells did not exhibit any protection against APAP-induced cytotoxicity. These cell lines also show enhanced cytotoxicity during MMI pretreatment.

DISCUSSION

The mechanism of APAP-induced cellular and liver organ toxicity is multifactorial and complex (Jaeschke and Bajt, 2006; Jaeschke *et al.*, 2012). Examining novel genes and pathways differentially regulated in experimental models of xenobiotic hep-

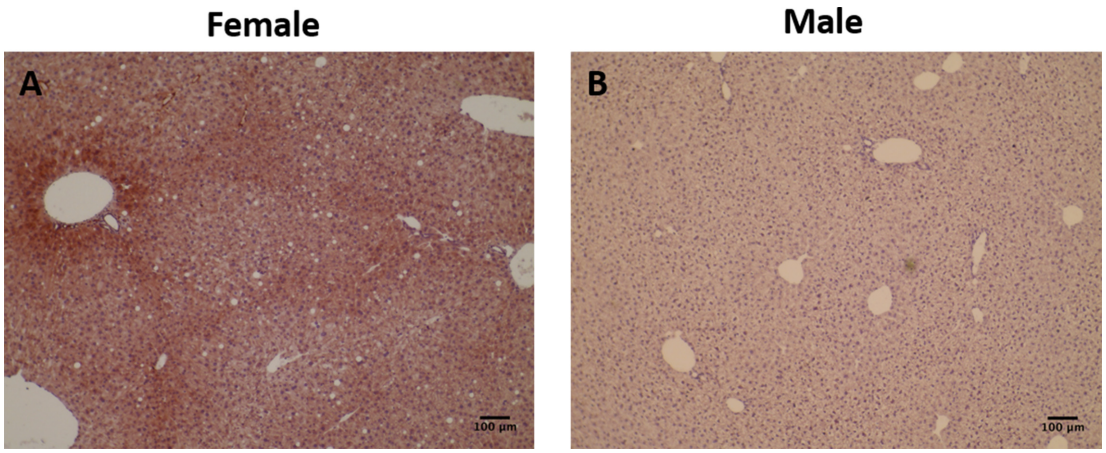

FIG. 7. Immunohistochemical analysis of Fmo3 in naïve female and male liver. Livers from untreated female and male mice were collected and fixed in zinc formalin and paraffin embedded. Immunochemical staining of Fmo3 was performed on paraffin sections using the custom-antibody used before. Representative images are shown. Scale bar: 100 µm. (A) Female; (B) male liver specimens.

TABLE 1 Histopathological Analysis of Livers after MMI Intervention in APAP-Treated Mice

Treatment group	Histological grade						>2 (%)
	0	1	2	3	4	5	
Control	5	0	0	0	0	0	0
APAP	0	5	0	0	0	0	0
1 and 2 MMI/APAP*#	0	0	0	1	1	2	100
1 MMI/APAP*	0	0	4	1	0	0	20
APAP/2 MMI	0	5	0	0	0	0	0

Note. Liver sections were examined for severity of degenerative and necrotic changes in centrilobular region as described previously (Manautou *et al*., 1994). Liver samples with grades >2 are considered to have significant injury. Data were rank ordered prior to statistical analysis. Asterisks (*) represent a statistical difference ($p < 0.05$) from vehicle control group and hash (#) represent a statistical difference ($p < 0.05$) from APAP-treated group.

atotoxicity resistance can provide novel avenues to develop new modalities of treatment for liver diseases. Our laboratory has previously developed a mouse model of APAP autoprotection for studying the mechanisms of hepatic injury/recovery (Aleksunes *et al*., 2008). This study also elucidated the role of efflux transporter MRP4 and compensatory cellular proliferation in protecting against APAP-induced hepatotoxicity in this model of APAP autoprotection. However, it is possible that factors other than MRP4 also can contribute to the development of APAP toxicity tolerance. A gene array analysis recently conducted in our lab provided insights into signaling pathways potentially involved in APAP autoprotection (O'Connor *et al*., 2014). *Fmo3* was among the genes with the most significant change in APAP autoprotected mice. Even though a role of *Fmo3* expression in APAP hepatotoxicity is not known, it was the most biologically plausible for playing a role in autoprotection.

In this study, we investigated the hepatic expression of Fmo3 protein during APAP-induced hepatotoxicity. Historically, Fmo3 was considered to be a noninducible drug-metabolizing enzyme (Cashman and Zhang, 2002, 2006; Hines, 2006; Krueger and Williams, 2005). However, recent studies show that activation of the Ah receptor induces Fmo3 mRNA levels (Celius *et al*., 2008, 2010). In these studies, although there is a very large increase in Fmo3 mRNA levels, protein levels measured by methimazole oxidation show only modest increases in protein function. Similarly, our results show that the dramatic elevation in liver Fmo3 mRNA expression following administration of a single APAP dose is accompanied by marginal increases in Fmo3 protein expression and catalytic activity. It is worth noting that the Fmo3 mRNA expression is variable between studies, which is again similar to the observations with ligand-dependent activation of AhR and Fmo3 mRNA expression (Celius *et al*., 2008). These differences in expression cannot be due to diurnal variation in basal expression because animals were dosed and tissue harvested at approximately the same time of the day every time we conducted independent studies. Fmo3 is subject to hormone regulation (Cherrington *et al*., 1998; Falls *et al*., 1997; Janmohamed *et al*., 2004), and such, 9- to 10-week-old mice were used in the current study. Irrespective of the level and degree of increased Fmo3 mRNA expression following a single dose APAP treatment, increases in protein expression remained marginal.

In contrast to what was observed with a single hepatotoxic APAP dose, both liver Fmo3 mRNA and protein expression are significantly higher in mice treated with the APAP autoprotection regimen (pre- and post-APAP treatments). In agreement with greater Fmo3 protein expression, Fmo3 catalytic activity and centrilobular zonal expression also are significantly greater in the APAP autoprotection group. These findings suggest the regulation of Fmo3 gene expression (transcriptional and/or translational) is different under the conditions of treatment with a single APAP dose versus an autoprotection treatment regimen. Because the level of damage from a mildly toxic

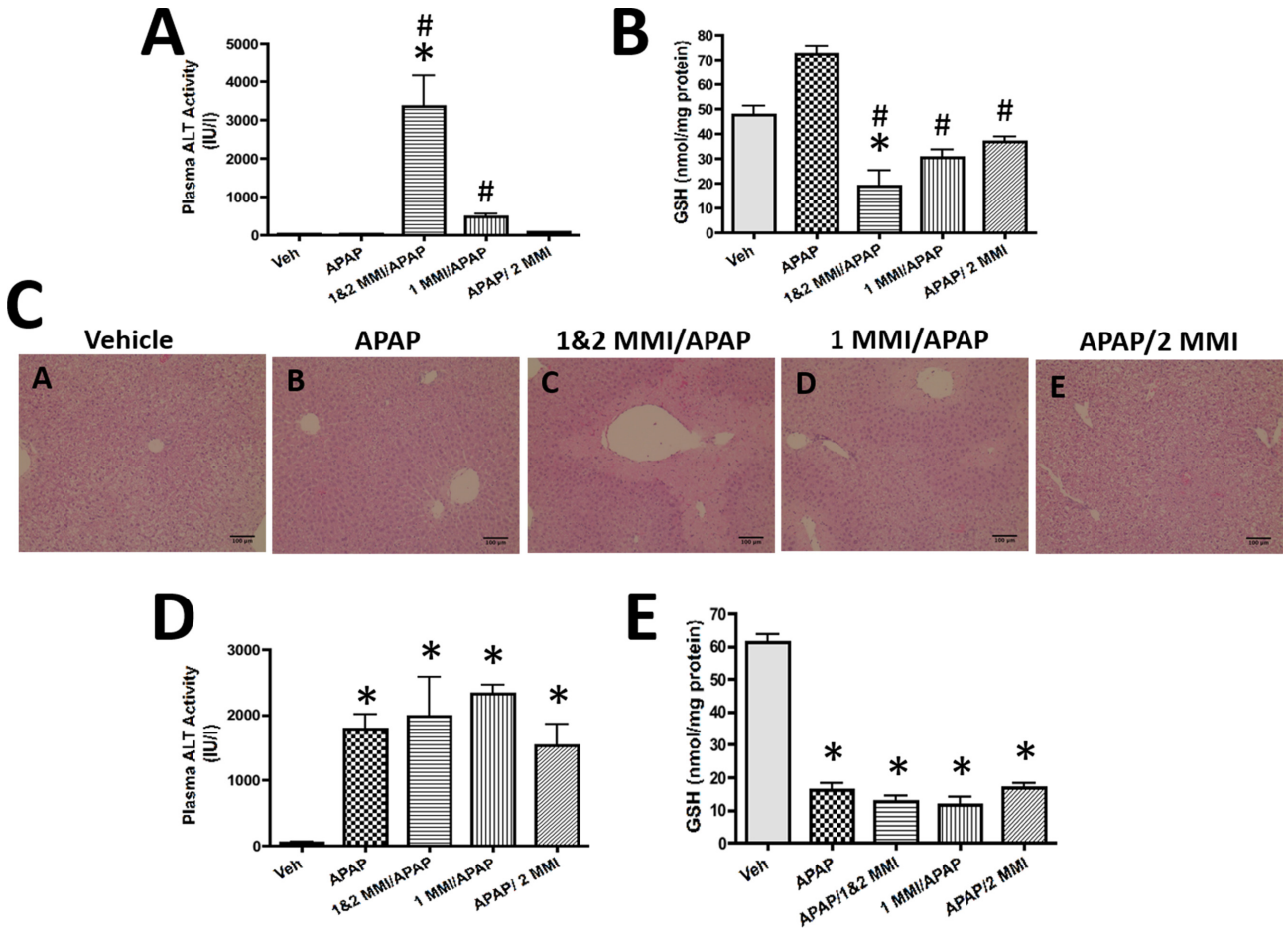

FIG. 8. Plasma ALT activity, hepatic GSH levels, and histopathology of liver sections after MMI intervention in APAP-treated mice. Female or male mice were treated with vehicle or APAP (400 mg/kg) or APAP along with MMI (50 mg/kg). The first dose of MMI was administered 30 min prior to APAP treatment and the second dose 12 h after the first dose. Twenty-four hours after APAP treatment, plasma and livers were collected for analysis. (A) The data from female mice are presented as mean plasma ALT (IU/l) ± SE. (B) GSH levels in female mice livers are expressed as GSH nmol/mg protein ± SE. One-way ANOVA was performed followed by the Dunnett's *post hoc* test. Asterisks (*) represent a statistical difference ($p < 0.05$) compared with vehicle-treated group and hash (#) represent a statistical difference ($p < 0.05$) from APAP-treated group. (C) Histopathology of formalin-fixed, paraffin-embedded liver sections after MMI intervention in APAP-treated female mice. Representative images are shown. Scale bar: 100 μm. (A) Vehicle: vehicle-treated group; (B) APAP: APAP (400 mg/kg)-treated group; (C) 1 and 2 MMI/APAP: APAP (400 mg/kg) with both the first and second dose MMI (50 mg/kg)-treated group; (D) 1 MMI/APAP: APAP (400 mg/kg) with the first dose MMI (50 mg/kg)-treated group; (E) APAP/2 MMI: APAP (400 mg/kg) with the second dose MMI (50 mg/kg)-treated group. (D) The data from male mice are presented as mean plasma ALT (IU/l) ± SE. (E) GSH levels in male mice livers are expressed as GSH nmol/mg protein ± SE. One-way ANOVA was performed followed by the Dunnett's *post hoc* test. Asterisks (*) represent a statistical difference ($p < 0.05$) compared with vehicle-treated group.

dose of APAP is minimal, the need for restoration of balance in cellular processes may also be less. Thus, all mRNA transcribed in response to the minimally toxic APAP exposure may not be translated into functional protein. In contrast, after an autoprotected dosing regimen, the initial exposure to a mildly toxic APAP dose would prime the tissue for faster recovery from reexposure to a second toxic insult. Indeed, the possibility exists that at least a portion of the dramatic increases in Fmo3 protein observed with the second APAP dose results from rapid translation of Fmo3 mRNA stabilized in ribonucleoprotein complexes. Such translational control has been well documented in other systems where a rapid response to a potentially toxic exposure occurs (e.g., translation of stored ferritin mRNA in response to iron exposure). This overall concept is well accepted and referred to by some scientists as "hormesis." The precise cellular and molecular events leading to this adaptation is not known. Moreover, immunohistochemical analysis of APAP autoprotected livers show the Fmo3 expression is localized to the hepatic centrilobular regions, where APAP-induced damage and/or hepatocellular compensatory repair/proliferation occurs, instead of the conventional periportal localization seen in female livers. This expression pattern is again suggestive of a potential Fmo3 role in the development of APAP hepatotoxicity resistance via an unknown cytoprotective function.

Female mice exhibit higher *Fmo3* gene expression than male mice (Cherrington *et al.*, 1998; Hines, 2006; Janmohamed *et al.*, 2004), and are much more resistant to APAP hepatotoxicity compared with males (Dai *et al.*, 2006). Our findings with the FMO inhibitor methimazole in female mice demonstrate that MMI inhibition of Fmo3 makes female mice susceptible to APAP-induced hepatotoxicity. The caveats of any inhibitor study are the specificity of inhibition as well as potential off target effects exhibiting toxicity comparable to that seen in males. Historically, MMI is known to interfere with the synthesis of thyroid hormones by inhibiting the enzyme, thyroperoxidase and is capable of inhibiting other enzymes involved in oxygenation reactions such as

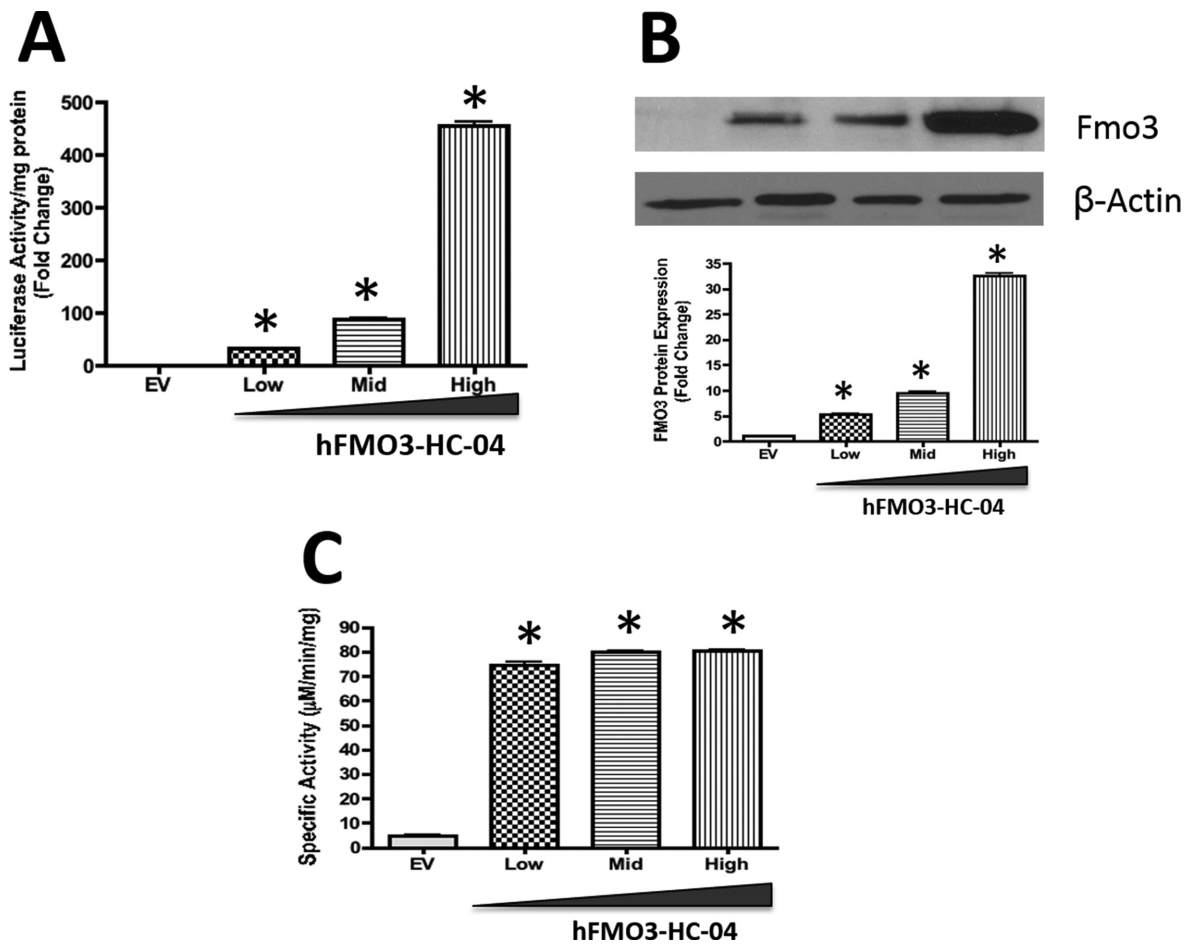

FIG. 9. Establishment of HC-04 cells over-expressing human FMO3 (hFMO3-HC-04). Lentiviral vector construction and transduction are described in detail in the Materials and Methods section. (A) Luciferase activity to measure the efficiency of transduction in hFMO3-HC-04 clones. The data are presented as mean luciferase activity/mg protein (fold change) ± SE. (B) Western blot for Fmo3 was performed using microsomal protein isolated from empty vector (EV), Low-, Mid-, and High-FMO3 expressing cell lines. Rabbit anti-human FMO3 primary antibody was used to detect FMO3 protein expression. Equal protein loading (10 μg protein/lane) was confirmed by detection of β-actin. The data are presented as blots as well as mean FMO3 protein expression (fold change) ± SE. (C) Microsomes isolated from EV expressing HC-04 cells and all three FMO3-over-expressing HC-04 clones were used to measure FMO activity using methimazole as substrate. Data are presented as mean specific activity (μM/min/mg) ± SE protein. One-way ANOVA was performed followed by the Dunnett's *post hoc* test. Asterisks (*) represent a statistical difference ($p < 0.05$) compared with EV controls.

FMO- and CYP-dependent monooxygenases (Hunter and Neal, 1975). If MMI was contributing to changing female mice susceptibility to APAP hepatotoxicity by inhibiting CYP-dependent metabolism, we would have anticipated seeing less liver damage. Clearly, this is not the case because MMI treatment makes female mice sensitive to APAP hepatotoxicity. This is quite remarkable because C57BL/6J female mice are quite resilient to APAP hepatotoxicity. Undesirable side effects such as cholestasis can develop from MMI treatment due to extrathyroidal actions in humans (Schmidt *et al.*, 1986). However, a cholestatic liver is less susceptible to APAP-induced hepatotoxicity in mice (Silva *et al.*, 2006). Lastly, MMI at higher doses can deplete hepatic GSH levels or in GSH-depleted mice induce centrilobular necrosis (Mizutani *et al.*, 1999, 2000). However, under the conditions used in the current study, MMI treatment alone does not result in GSH depletion or hepatotoxicity in mice. Furthermore, MMI treatment in male mice did not alter APAP-induced hepatotoxicity negating any potential nonspecific functions of MMI. Collectively, these results suggest that the susceptibility of female mice to APAP hepatotoxicity following MMI treatment is the result of inhibiting Fmo3 function.

To further study the importance of FMO3 over-expression, we established an *in vitro* over-expression system using HC-04 cells. Although the percentage LDH leakage into the media in Low-FMO3 expressing hFMO3-HC-04 cells in response to APAP treatment is significantly lower compared with empty vector controls, the amount of LDH leakage by APAP does not change in the Mid-FMO3 expressing clone and is significantly greater in High-FMO3 cells. Taken together, these data suggest that over-expression of FMO3 significantly alters susceptibility to APAP-induced cytotoxicity. Even though the percentage protection from APAP cytotoxicity in the Low-FMO3 expressing clone is only ~20%, one must keep in mind that FMO3 over-expressing cells are a mono cell culture. The possible contribution from other cell types, such as Kupffer cells and endothelial cells known to play an important role in signaling mechanisms should not be overlooked. The data also suggest that there is a threshold for FMO3 over-expression in protecting against APAP-induced cytotoxicity. This is evidenced by the enhanced APAP cytotoxicity in the High-expressing FMO3 cells. MMI treatment did not result in elevation of basal LDH leakage into the medium in all FMO3-over-expressing clones (data not shown). This suggests that MMI

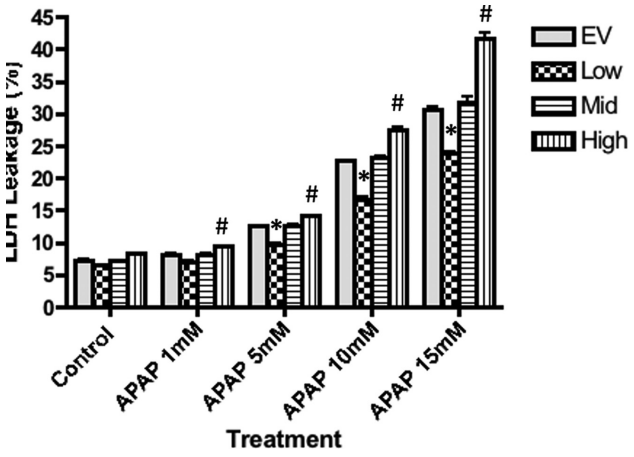

FIG. 10. Effect of APAP treatment in HC-04 cells overexpressing human FMO3 (hFMO3-HC-04). Empty vector, Low-, Mid-, and High-FMO3 expressing cell lines were treated with a range of APAP concentrations from 1 to 15mM. Twenty-four hours later, percentage LDH leakage into the medium was measured using a commercial kit. The data are presented as mean LDH leakage (%) ± SE. Two-way ANOVA was performed followed by the Bonferroni's *post hoc* test. Asterisks (*) represent a significant decrease ($p < 0.05$) compared with EV controls and hash (#) represent a significant increase ($p < 0.05$) compared with EV controls.

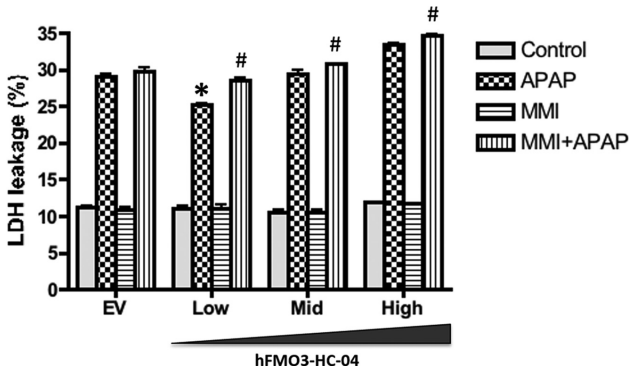

FIG. 11. Effect of MMI pretreatment during APAP-induced cytotoxicity in HC-04 cells over-expressing human FMO3 (hFMO3-HC-04). Empty vector, Low-, Mid-, and High-FMO3 expressing cell lines were incubated with MMI (1 mM) for 30 min before APAP (15 mM) treatment. Twenty-four hours after APAP treatment, percentage LDH leakage into the medium was measured. The data are presented as mean LDH leakage (%) ± SE. Two-way ANOVA was performed followed by the Bonferroni's *post hoc* test. Asterisks (*) represent a significant decrease ($p < 0.05$) compared with APAP-treated EV control and hash (#) represent a significant increase ($p < 0.05$) compared with respective APAP-treated EV and hFMO3-HC-04 cell lines.

by itself at doses used *in vitro* did not result in cytotoxicity. Inhibition of FMO3 activity by MMI in all three Low-, Mid-, and High-FMO3 expressing cell lines resulted in rescue of sensitivity to APAP in Low-FMO3 expressing cell line compared with EV controls. Because High-FMO3 expressing cells exhibit greater LDH leakage in comparison to EV controls following APAP treatment (threshold for FMO3 over-expression), one might anticipate seeing lower APAP cytotoxicity following MMI cotreatment. Considering this is not the case, it is possible that MMI at 1 mM concentration results in inhibition of FMO3 activity in Low-FMO3 expressing cell line but is metabolized in High-FMO3 expressing cells. To emphasize, MMI is a substrate for Fmo3 as well as a competitive inhibitor with IC_{50} value of 60.2 ± 16.2 μM (Attar *et al.*, 2003; Rettie and Fisher, 1999).

FMO is involved in oxygenation of phosphorus, nitrogen, and sulfur-containing xenobiotics. FMOs also are involved in the oxidation of endogenous substrates such as cysteamine to cystamine (Poulsen, 1981). Although the physiological role of FMO3 cysteamine S-oxygenation is not clear, Zieglar and Poulsen proposed in the 1970s that FMO might be involved in protein disulfide bond formation through oxidation of cysteamine. It was also proposed that oxygenation of cysteamine may be a significant source of disulfide, maintaining the cellular thiol:disulfide potential in a cell (Ziegler *et al.*, 1979). Further, Suh and Robertus (2002) showed that yeast FMO serve as a modulator of cellular thiols and maintains optimum redox potential within the endoplasmic reticulum, allowing for proper folding of disulfide bond-containing proteins (Suh and Robertus, 2002). The cytoprotective functions of Fmo3 and its possible involvement in APAP autoprotection are summarized below. The relationship between cellular thiol:disulfide ratios and the regulation of metabolic reactions has been recognized for a long time (Barron, 1953). Oxygenation of cysteamine during APAP hepatotoxicity may serve to help control the overall thiol:disulfide redox state of the cell, which in turn may modulate cellular metabolism and/or activate signal transduction pathway leading to altered susceptibility to APAP (or protection). Oxygenation of cysteamine to cystamine by Fmo3 and transport out of the cell also may represent a detoxication mechanism or protective function, because cysteamine is toxic to cells at concentrations as low as 39 μM through the transition metal-dependent formation of hydrogen peroxide (Jeitner and Lawrence, 2001). To investigate whether oxygenation of cysteamine to cystamine by Fmo3 is important during APAP hepatotoxicity, follow-up studies will measure the total hepatic cysteamine and cystamine concentrations in the mouse model of APAP autoprotection.

In the present study, up-regulation of *Fmo3* gene expression in the mouse APAP autoprotection model and its role in protecting against APAP-induced cytotoxicity or hepatotoxicity has led to the conclusion that Fmo3 is important for development of resistance to APAP-induced hepatotoxicity. The phenomenon of autoprotection is also seen in patients who are repeatedly exposed to supratherapeutic doses of APAP (Shayiq *et al.*, 1999; Watkins *et al.*, 2006). These clinical data suggest that human liver can adapt to APAP-induced hepatotoxicity similar to that seen in our APAP autoprotection mouse model. C57BL/6J wild-type mice are commonly used for studies of APAP hepatotoxicity and the mechanisms of toxicity in these animals are not yet completely understood. Although, key events such as NAPQI formation, GSH depletion, protein arylation, peroxynitrate formation, and mitochondrial damage have been demonstrated to play an important role in APAP hepatotoxicity (Cohen *et al.*, 1997; Hinson *et al.*, 2010; Jaeschke and Bajt, 2006; Jaeschke *et al.*, 2011; McGill *et al.*, 2012). Even though primary human hepatocytes are the gold standard tool for studying APAP hepatotoxicity mechanisms, they have major drawbacks. The availability of these cells is limited, and the drug response can vary significantly due to differences in donors. Most importantly, the lifespan of primary human hepatocytes is short and they undergo changes in CYP expression levels over time in culture. Hepatoma cell lines like HepG2 express very low CYP levels compared with primary human hepatocytes or human liver especially those that are involved in the metabolism of APAP (Rodriguez-Antona *et al.*, 2002). Using the more recently available human hepatoma cell line, HepaRG, which expresses a more normal spectrum of drug metabolizing enzymes, studies have demonstrated that the mechanistic features of APAP-induced hepatotoxicity are the same as reported for human hepatocytes and mouse liver *in vivo* (McGill

et al., 2011). Thus, it is very likely that the phenomenon of APAP autoprotection seen in human might also involve FMO3 overexpression. Although this is a subject of current investigation in our laboratory the mere fact that the protein once thought to be noninducible is being induced following treatment with a commonly used, over-the-counter drug-like acetaminophen is quite alarming. Importantly, one also must be concerned about the number of other drugs that are co-administered with APAP and are FMO3 substrates.

FUNDING

National Institutes of Health Grant (DK069557).

ACKNOWLEDGMENTS

An earlier version of this manuscript was submitted to the 2014 Society of Toxicology Mechanisms Specialty Section Carl C. Smith Graduate Student Award competition. Swetha Rudraiah was among the top 10 finalists and the recipient of the third place award.

REFERENCES

Aleksunes, L. M., Campion, S. N., Goedken, M. J. and Manautou, J. E. (2008). Acquired resistance to acetaminophen hepatotoxicity is associated with induction of multidrug resistance-associated protein 4 (Mrp4) in proliferating hepatocytes. *Toxicol. Sci.*, **104**, 261–273.

Attar, M., Dong, D., Ling, K. H. and Tang-Liu, D. D. (2003). Cytochrome P450 2C8 and flavin-containing monooxygenases are involved in the metabolism of tazarotenic acid in humans. *Drug Metab. Dispos.*, **31**, 476–481.

Barron, E. S. (1953). The importance of sulfhydryl groups in biology and medicine. *Tex. Rep. Biol. Med.*, **11**, 653–670.

Cashman, J. R. and Hanzlik, R. P. (1981). Microsomal oxidation of thiobenzamide. A photometric assay for the flavin-containing monooxygenase. *Biochem. Biophys. Res. Commun.*, **98**, 147–153.

Cashman, J. R. and Zhang, J. (2002). Interindividual differences of human flavin-containing monooxygenase 3: Genetic polymorphisms and functional variation. *Drug Metab. Dispos.*, **30**, 1043–1052.

Cashman, J. R. and Zhang, J. (2006). Human flavin-containing monooxygenases. *Annu. Rev. Pharmacol. Toxicol.*, **46**, 65–100.

Celius, T., Pansoy, A., Matthews, J., Okey, A. B., Henderson, M. C., Krueger, S. K. and Williams, D. E. (2010). Flavin-containing monooxygenase-3: Induction by 3-methylcholanthrene and complex regulation by xenobiotic chemicals in hepatoma cells and mouse liver. *Toxicol. Appl. Pharmacol.*, **247**, 60–69.

Celius, T., Roblin, S., Harper, P. A., Matthews, J., Boutros, P. C., Pohjanvirta, R. and Okey, A. B. (2008). Aryl hydrocarbon receptor-dependent induction of flavin-containing monooxygenase mRNAs in mouse liver. *Drug Metab. Dispos.*, **36**, 2499–2505.

Cherrington, N. J., Cao, Y., Cherrington, J. W., Rose, R. L. and Hodgson, E. (1998). Physiological factors affecting protein expression of flavin-containing monooxygenases 1, 3 and 5. *Xenobiotica*, **28**, 673–682.

Cohen, S. D., Pumford, N. R., Khairallah, E. A., Boekelheide, K., Pohl, L. R., Amouzadeh, H. R. and Hinson, J. A. (1997). Selective protein covalent binding and target organ toxicity. *Toxicol. Appl. Pharmacol.*, **143**, 1–12.

Dai, G., He, L., Chou, N. and Wan, Y. J. (2006). Acetaminophen metabolism does not contribute to gender difference in its hepatotoxicity in mouse. *Toxicol. Sci.*, **92**, 33–41.

Falls, J. G., Cherrington, N. J., Clements, K. M., Philpot, R. M., Levi, P. E., Rose, R. L. and Hodgson, E. (1997). Molecular cloning, sequencing, and expression in escherichia coli of mouse flavin-containing monooxygenase 3 (FMO3): Comparison with the human isoform. *Arch. Biochem. Biophys.*, **347**, 9–18.

Hernandez, D., Janmohamed, A., Chandan, P., Omar, B. A., Phillips, I. R. and Shephard, E. A. (2009). Deletion of the mouse Fmo1 gene results in enhanced pharmacological behavioural responses to imipramine. *Pharmacogenet. Genomics*, **19**, 289–299.

Hines, R. N. (2006). Developmental and tissue-specific expression of human flavin-containing monooxygenases 1 and 3. *Expert Opin. Drug Metab. Toxicol.*, **2**, 41–49.

Hinson, J. A., Roberts, D. W. and James, L. P. (2010). Mechanisms of acetaminophen-induced liver necrosis. *Handb. Exp. Pharmacol.*, **196**, 369–405.

Hunter, A. L. and Neal, R. A. (1975). Inhibition of hepatic mixed-function oxidase activity in vitro and in vivo by various thiono-sulfur-containing compounds. *Biochem. Pharmacol.*, **24**, 2199–2205.

Jaeschke, H. and Bajt, M. L. (2006). Intracellular signaling mechanisms of acetaminophen-induced liver cell death. *Toxicol. Sci.*, **89**, 31–41.

Jaeschke, H., McGill, M. R. and Ramachandran, A. (2012). Oxidant stress, mitochondria, and cell death mechanisms in drug-induced liver injury: Lessons learned from acetaminophen hepatotoxicity. *Drug Metab. Rev.*, **44**, 88–106.

Jaeschke, H., McGill, M. R., Williams, C. D. and Ramachandran, A. (2011). Current issues with acetaminophen hepatotoxicity–a clinically relevant model to test the efficacy of natural products. *Life Sci.*, **88**, 737–745.

Janmohamed, A., Hernandez, D., Phillips, I. R. and Shephard, E. A. (2004). Cell-, tissue-, sex- and developmental stage-specific expression of mouse flavin-containing monooxygenases (fmos). *Biochem. Pharmacol.*, **68**, 73–83.

Jeitner, T. M. and Lawrence, D. A. (2001). Mechanisms for the cytotoxicity of cysteamine. *Toxicol. Sci.*, **63**, 57–64.

Koukouritaki, S. B., Simpson, P., Yeung, C. K., Rettie, A. E. and Hines, R. N. (2002). Human hepatic flavin-containing monooxygenases 1 (FMO1) and 3 (FMO3) developmental expression. *Pediatr. Res.*, **51**, 236–243.

Krueger, S. K. and Williams, D. E. (2005). Mammalian flavin-containing monooxygenases: Structure/function, genetic polymorphisms and role in drug metabolism. *Pharmacol. Ther.*, **106**, 357–387.

Larson, A. M., Polson, J., Fontana, R. J., Davern, T. J., Lalani, E., Hynan, L. S. and Acute Liver Failure Study Group. (2005). Acetaminophen-induced acute liver failure: Results of a united states multicenter, prospective study. *Hepatology*, **42**, 1364–1372.

Lee, W. M. (2010). The case for limiting acetaminophen-related deaths: Smaller doses and unbundling the opioid-acetaminophen compounds. *Clin. Pharmacol. Ther.*, **88**, 289–292.

Lim, P. L., Tan, W., Latchoumycandane, C., Mok, W. C., Khoo, Y. M., Lee, H. S. and Boelsterli, U. A. (2007). *Molecular and functional characterization of drug-metabolizing enzymes and transporter expression in the novel spontaneously immortalized human hepatocyte line HC-04. Toxicol. In Vitro*, **21**, 1390–1401.

Maherali, N., Ahfeldt, T., Rigamonti, A., Utikal, J., Cowan, C. and Hochedlinger, K. (2008). A high-efficiency system for the generation and study of human induced pluripotent stem cells.

Cell Stem Cell, **3**, 340–345.

Manautou, J. E., Hoivik, D. J., Tveit, A., Hart, S. G., Khairallah, E. A. and Cohen, S. D. (1994). Clofibrate pretreatment diminishes acetaminophen's selective covalent binding and hepatotoxicity. *Toxicol. Appl. Pharmacol.*, **129**, 252–263.

McGill, M. R., Williams, C. D., Xie, Y., Ramachandran, A. and Jaeschke, H. (2012). Acetaminophen-induced liver injury in rats and mice: Comparison of protein adducts, mitochondrial dysfunction, and oxidative stress in the mechanism of toxicity. *Toxicol. Appl. Pharmacol.*, **264**, 387–394.

McGill, M. R., Yan, H. M., Ramachandran, A., Murray, G. J., Rollins, D. E. and Jaeschke, H. (2011). HepaRG cells: A human model to study mechanisms of acetaminophen hepatotoxicity. *Hepatology*, **53**, 974–982.

Mizutani, T., Murakami, M., Shirai, M., Tanaka, M. and Nakanishi, K. (1999). Metabolism-dependent hepatotoxicity of methimazole in mice depleted of glutathione. *J. Appl. Toxicol.*, **19**, 193–198.

Mizutani, T., Yoshida, K., Murakami, M., Shirai, M. and Kawazoe, S. (2000). Evidence for the involvement of N-methylthiourea, a ring cleavage metabolite, in the hepatotoxicity of methimazole in glutathione-depleted mice: Structure-toxicity and metabolic studies. *Chem. Res. Toxicol.*, **13**, 170–176.

Moffit, J. S., Koza-Taylor, P. H., Holland, R. D., Thibodeau, M. S., Beger, R. D., Lawton, M. P. and Manautou, J. E. (2007). Differential gene expression in mouse liver associated with the hepatoprotective effect of clofibrate. *Toxicol. Appl. Pharmacol.*, **222**, 169–179.

Nace, C. G., Genter, M. B., Sayre, L. M. and Crofton, K. M. (1997). Effect of methimazole, an FMO substrate and competitive inhibitor, on the neurotoxicity of 3,3′-iminodipropionitrile in male rats. *Fundam. Appl. Toxicol.*, **37**, 131–140.

O'Connor, M. A., Koza-Taylor, P., Campion, S. N., Aleksunes, L. M., Gu, X., Enayetallah, A. E. and Manautou, J. E. (2014). Analysis of changes in hepatic gene expression in a murine model of tolerance to acetaminophen hepatotoxicity (autoprotection). *Toxicol. Appl. Pharmacol.*, **274**, 156–167.

Overby, L. H., Buckpitt, A. R., Lawton, M. P., Atta-Asafo-Adjei, E., Schulze, J. and Philpot, R. M. (1995). Characterization of flavin-containing monooxygenase 5 (FMO5) cloned from human and guinea pig: Evidence that the unique catalytic properties of FMO5 are not confined to the rabbit ortholog. *Arch. Biochem. Biophys.*, **317**, 275–284.

Poulsen, L. L. (1981). In *Reviews in Biochemical Toxicology* (E. Hodgson, J. R. Bend and R. M. Philpot, Eds.), pp. 33–49. Elsevier Press, North Holland.

Rahman, I., Kode, A. and Biswas, S. K. (2006). Assay for quantitative determination of glutathione and glutathione disulfide levels using enzymatic recycling method. *Nat. Protoc.*, **1**, 3159–3165.

Rettie, A. E. and Fisher, M. B. (1999). *Handbook of drug metabolism*. In *Transformation Enzymes: Oxidative; Non-P450* (T. F. Woolf, Ed.), pp. 132. Marcel Dekker, Inc., New York.

Rodriguez-Antona, C., Donato, M. T., Boobis, A., Edwards, R. J., Watts, P. S., Castell, J. V. and Gomez-Lechon, M. J. (2002). Cytochrome P450 expression in human hepatocytes and hepatoma cell lines: Molecular mechanisms that determine lower expression in cultured cells. *Xenobiotica*, **32**, 505–520.

Schmidt, G., Borsch, G., Muller, K. M. and Wegener, M. (1986). Methimazole-associated cholestatic liver injury: Case report and brief literature review. *Hepato-Gastroenterology*, **33**, 244–246.

Shayiq, R. M., Roberts, D. W., Rothstein, K., Snawder, J. E., Benson, W., Ma, X. and Black, M. (1999). Repeat exposure to incremental doses of acetaminophen provides protection against acetaminophen-induced lethality in mice: An explanation for high acetaminophen dosage in humans without hepatic injury. *Hepatology*, **29**, 451–463.

Shephard, E. A. and Phillips, I. R. (2010). The potential of knockout mouse lines in defining the role of flavin-containing monooxygenases in drug metabolism. *Expert Opin. Drug Metab. Toxicol.*, **6**, 1083–1094.

Silva, V. M., Hennig, G. E. and Manautou, J. E. (2006). Cholestasis induced by model organic anions protects from acetaminophen hepatotoxicity in male CD-1 mice. *Toxicol. Lett.*, **160**, 204–211.

Suh, J. K. and Robertus, J. D. (2002). Role of yeast flavin-containing monooxygenase in maintenance of thiol-disulfide redox potential. *Methods Enzymol.*, **348**, 113–121.

Szymczak, A. L., Workman, C. J., Wang, Y., Vignali, K. M., Dilioglou, S., Vanin, E. F. and Vignali, D. A. (2004). Correction of multi-gene deficiency in vivo using a single 'self-cleaving' 2A peptide-based retroviral vector. *Nat. Biotechnol.*, **22**, 589–594.

Thakore, K. N. and Mehendale, H. M. (1991). Role of hepatocellular regeneration in CCl4 autoprotection. *Toxicol. Pathol.*, **19**, 47–58.

Watkins, P. B., Kaplowitz, N., Slattery, J. T., Colonese, C. R., Colucci, S. V., Stewart, P. W. and Harris, S. C. (2006). Aminotransferase elevations in healthy adults receiving 4 grams of acetaminophen daily: A randomized controlled trial. *JAMA*, **296**, 87–93.

Zhang, J., Cerny, M. A., Lawson, M., Mosadeghi, R. and Cashman, J. R. (2007). Functional activity of the mouse flavin-containing monooxygenase forms 1, 3, and 5. *J. Biochem. Mol. Toxicol.*, **21**, 206–215.

Ziegler, D. M., Duffel, M. W. and Poulsen, L. L. (1979). Studies on the nature and regulation of the cellular thio:Disulphide potential. *Ciba Found. Symp.*, 72, 191–204.